

**Supplementary Information**  
**for**  
**Biophysical interactions between self-sufficient cytochrome P450**  
**from *Tepidiphilus thermophilus* and ilaprazole**

Jaejeong You,<sup>a†</sup> Yunha Hwang,<sup>a†</sup> Yeon-Ju Jeong,<sup>b</sup> Soo-Jin Yeom,<sup>b,c</sup> Chul ho Yun,<sup>b,c</sup> Hyun Goo Kang<sup>\*d</sup>  
and Seung Jae Lee<sup>\*a,e</sup>

<sup>a</sup>Department of Chemistry, Jeonbuk National University, Jeonju 54896, Republic of Korea

<sup>b</sup>School of Biological Sciences and Technology, Graduate School, Chonnam National University, Gwangju 61186, Republic of Korea

<sup>c</sup>School of Biological Sciences and Technology, Chonnam National University, Gwangju 61186, Republic of Korea

<sup>d</sup>Department of Neurology and Research Institute of Clinical Medicine, Jeonbuk National University, Jeonju 54896, Republic of Korea

<sup>e</sup>Research Institute for the Molecular Biology and Genetics, Jeonbuk National University, Jeonju 54896, Republic of Korea

†These authors contributed equally to this work.

\*To whom correspondence should be addressed: hgkang@jbnu.ac.kr and slee026@jbnu.ac.kr

## Table of Contents

### Experimental

Materials and chemicals	S3
Expression of <i>Tepidiphilus thermophilus</i> CYP116B46	S3
Purification of <i>T. thermophilus</i> CYP116B46	S4
Measurement of binding affinities between CYP116B46 and ilaprazole	S4
Molecular docking simulation between CYP116B46 and ilaprazole	S5
<b>Figure S1</b> Metabolism of ilaprazole in human liver microsomes	S6
<b>Figure S2</b> Amino acid sequences of <i>T. thermophilus</i> CYP116B46	S7
<b>Figure S3</b> Sequence alignment of heme domain in <i>T. thermophilus</i> CYP116B46	S8
<b>Figure S4</b> Interaction of CYP116B46 with ilaprazole based on tryptophan quenching	S9
<b>Figure S5</b> Binding affinities between CYP116B46 and ilaprazole	S10
<b>Figure S6</b> Analysis of cavities in CYP450s	S11
<b>Figure S7</b> Overall docking models of CYP116B46 and ilaprazole	S12
<b>Table S1</b> Binding affinities and RMSD for docking models of CYP116B46 and ilaprazole	S13
<b>References</b>	S14

## Experimental

### Materials and chemicals

All chemicals and solvents used in protein expression were purchased from Sigma-Aldrich (St. Louis, MO, USA). Tris(hydroxymethyl)aminomethane (Tris; Daejung, Siheung, Republic of Korea), sodium chloride (NaCl; Daejung), dithiothreitol (DTT; GoldBio, St. Louis, MO, USA), glycerol (Samchun Chemical, Seoul, Republic of Korea), DNase I (Takara Bio, Shiga, Japan), phenylmethylsulfonyl fluoride (PMSF; Thermo Fisher Scientific, Waltham, MA, USA), and EDTA-free protease inhibitor cocktail (Roche Diagnostics GmbH, Mannheim, Germany) were used in protein purification. Buffer solutions were prepared using 3-(N-morpholino) propanesulfonic acid (MOPS; Thermo Fisher Scientific), 2-(N-morpholino) ethanesulfonic acid (MES; Sigma-Aldrich), and sodium acetate (Sigma-Aldrich). Fast protein liquid chromatography (FPLC; ÄKTA Pure 25 L, Cytiva, Marlborough, MA, USA) and an Econo-column (Bio-Rad Laboratories, Hercules, CA, USA) along with Ni-Sepharose (Cytiva) and Superdex 200 (Cytiva) were used in protein purification. An ultracentrifuge (Hanil Science, Gimpo, Republic of Korea) and bench-top centrifuge (Beckman Coulter, Brea, CA, USA) were used for separating cell debris and supernatant.

### Expression of *Tepidiphilus thermophilus* CYP116B46

The DNA sequence of CYP116B46 from *Tepidiphilus thermophilus* (*T. thermophilus*) was ligated into the pET-28a(+) vector. This vector was transformed into *Escherichia coli* C2566 (New England BioLabs, Hitchin, UK) cultured in kanamycin (50  $\mu\text{g mL}^{-1}$ )-containing Luria Bertani broth (250 mL) at 37 °C with shaking at 200 rpm for 16 h. The culture was scaled-up using kanamycin (50  $\mu\text{g mL}^{-1}$ )-containing terrific broth media (500 mL) supplemented with 1.0 mM thiamine, 0.025% (v/v) trace element solution, 50  $\mu\text{M}$   $\text{FeCl}_3 \cdot 6\text{H}_2\text{O}$ , 1.0 mM  $\text{MgCl}_2 \cdot 6\text{H}_2\text{O}$ , and 2.5 mM  $(\text{NH}_4)_2\text{SO}_4$ .<sup>1</sup> Incubation was performed at 37 °C and 200-rpm shaking until reaching an optical density at 600 nm ( $\text{OD}_{600}$ ) of 0.8–1.0. The whole culture was cooled to 26 °C and treated with 0.5 mM isopropyl- $\beta$ -D-thiogalactopyranoside and 1.5 mM  $\delta$ -aminolevulinic acid ( $\delta$ -ALA) to induce CYP116B46 expression with shaking at 150 rpm for 20 h. CYP116B46 was overexpressed until the concentration of CtCYP116B reached 0.20  $\mu\text{M}$ , as determined by the CO-bound difference spectrum at an extinction coefficient ( $\epsilon_{450-490}$ ) of 91,000  $\text{M}^{-1} \text{cm}^{-1}$ , and harvested via centrifugation at 13,000 rpm and 4 °C for 30 min.<sup>2</sup>

### **Purification of *T. thermophilus* CYP116B46**

The cell pellet obtained from overexpressed CYP116B46 (1 L) was dissolved in buffer A (20 mM Tris-HCl, 300 mM NaCl, 10 mM imidazole, 0.01  $\mu\text{L}/\text{mL}$  DNase I, 0.002 mg/mL PMSF, and EDTA-free Protease Inhibitor Cocktail at pH 8.0), sonicated for 60 min (15s on and 45 s off), and the supernatant was filtered through a 0.22- $\mu\text{m}$  membrane syringe filter (Sartorius). The Ni-Sepharose in the gravity column was equilibrated with buffer B (20 mM Tris-HCl, 300 mM NaCl, 10 mM imidazole at pH 8.0) before applying the supernatant at 4 °C and 200 rpm for 12–16 h. The flow-through was collected under argon gas with imidazole (50, 100, 150, 200, 250, and 300 mM)-containing buffer B. The eluates were analyzed using sodium dodecyl sulfate-polyacrylamide gel electrophoresis, and the target eluates were concentrated via filtration through a 30-kDa membrane filter (Merck Millipore) with centrifugation at 4 °C and 3,000 rpm. The concentrated eluates were applied in the second purification using the Superdex-200 column on the FPLC system, which was activated using buffer C (25 mM Tris-HCl, 50 mM NaCl, 1 mM DTT, and 5% glycerol at pH 8.0). The target eluates were concentrated via filtration through a 30-kDa membrane filter with centrifugation at 4 °C and 3,000 rpm. The concentration of CYP116B46 was calculated at  $\epsilon_{418} = 121 \text{ mM}^{-1} \text{ cm}^{-1}$  for the solet peak of the oxidized enzyme using a UV-Vis spectrophotometer (Cary 3500, Agilent Technologies, Santa Clara, CA, USA) and stored at  $-88 \text{ }^\circ\text{C}$  for subsequent experiments.<sup>3</sup>

### **Measurement of binding affinities between CYP116B46 and ilaprazole**

The binding affinities ( $K_{\text{d}}$ s) between CYP116B46 and ilaprazole were measured using a spectrofluorometer (FP-8300, JASCO, Tokyo, Japan) through tryptophan quenching at 282 nm ( $\lambda_{\text{ex}}$ ) and 336 nm ( $\lambda_{\text{em}}$ ).<sup>4,5</sup> All experiments were performed at a bandwidth of 2.5 nm, response of 1 s, PMT voltage of 800 V, and 25 °C. One equivalent of CYP116B46 ( $2.56 \times 10^{-10}$  mol) in buffer D (25 mM buffer; *vide infra*, 50 mM NaCl, 1 mM DTT) was titrated in a cuvette (J/3 type material Q, JASCO) with ilaprazole to saturation (~60 equivalents). The experiments were conducted in buffer D adjusted to various pH levels using 25 mM buffers: Tris-HCl (pH 8.0 or 7.0), MOPS (pH 6.0), MES (pH 5.0), and sodium acetate (pH 4.0 or 3.0). The changes in fluorescence intensity were curve-fitted using the 1:n binding model (Hill equation) to estimate  $K_{\text{d}}$ s using Origin 2018 (OriginLab, Northampton, MA, USA), as represented by the following equation:

$$F_{332} = \text{Start} + (\text{End} - \text{Start}) \times \frac{I_{\text{total}}^n}{(K_{\text{d}}^n + I_{\text{total}}^n)}$$

$F_{332}$ : Fluorescence intensity at 332 nm

Start: Initial fluorescence intensity at 332 nm

End: Saturated fluorescence intensity at 332 nm

I: Concentration of ilaprazole

$K_d$ : Dissociation constant

n: Hill coefficient

### **Molecular docking simulation between CYP116B46 and ilaprazole**

The docking of ilaprazole with CYP116B46 was simulated using AutoDock Vina.<sup>6</sup> The structure of Ilaprazole was optimized through MMFF94 energy minimization in ChemBio3D Ultra 11.0.<sup>7</sup> Structural files for both ilaprazole and CYP116B46 were generated using AutoDock Tools and then imported into PyRx for simulation.<sup>8</sup> The search space covered the entire CYP116B46 protein (PDB ID: 6GII), and the exhaustiveness parameter was set to 1024 to ensure a comprehensive search.<sup>9</sup> The docked structures of CYP116B46 and ilaprazole were analyzed using PyMol v3.0.3.<sup>10</sup> Binding energies were converted into dissociation constant ( $K_d$ ) values using the following equation<sup>11</sup>:

$$\Delta G_{binding} = RT \ln K_d$$

$\Delta G_{binding}$ : Free binding energy

R: Gas constant; 8.314 J/(mol·K)

T: Temperature; 298 K (at 25 °C)

$K_d$ : Dissociation constant

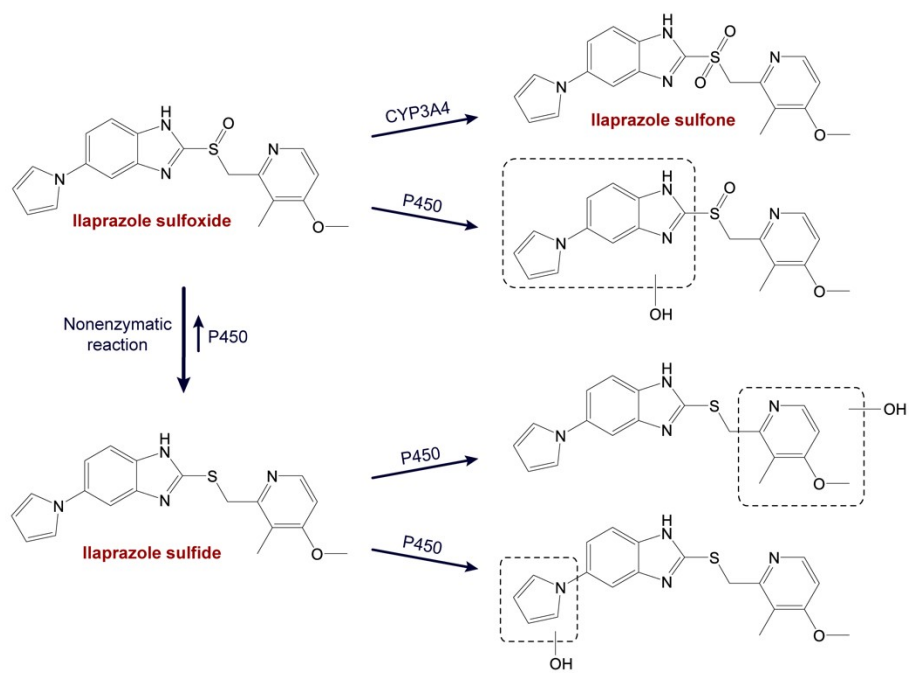


**Figure S1.** Metabolism of ilaprazole in human liver microsomes.<sup>12</sup>

<sup>1</sup>METELKETARGTCPVAHGGQSSVGGCPVHRLAEDFDPFQDAYMADPAQFV<sup>130</sup>VRWAREQVPIF  
Cytochrome P450 130  
YAPKLN<sup>135</sup>YWVVTRYDTIKQIFRDPVTFSPSNV<sup>140</sup>LQSF<sup>145</sup>AQPSAEVRQVLERYGYAFNRT<sup>150</sup>LVNE  
DEPM<sup>155</sup>H<sup>160</sup>L<sup>165</sup>ER<sup>170</sup>RRVLM<sup>175</sup>EPFASEHLAEHEP<sup>180</sup>MVREL<sup>185</sup>VRR<sup>190</sup>AVNRFIDTGRADLVDQMIWEVPFTVA  
LHFLGVDDDDREKMRRFAIAHTVNAFGRPSPEEQ<sup>195</sup>LAVAETV<sup>200</sup>GQFWQFCGEVLEKMRRTAD  
GPGWMRYSIRQ<sup>205</sup>QKLYPDVVTDSYLHSM<sup>210</sup>QAI<sup>215</sup>IV<sup>220</sup>AAHETTVFATTNALKTLL<sup>225</sup>EHETVWREI  
CADPSLI<sup>230</sup>PAAAE<sup>235</sup>CL<sup>240</sup>RYNG<sup>245</sup>PVAG<sup>250</sup>WRRRTT<sup>255</sup>REVEVEGVRLPVGANILMV<sup>260</sup>VAS<sup>265</sup>NHDSAHFD  
DPEFFDIGRSNASEHL<sup>270</sup>NFGYGA<sup>275</sup>HQ<sup>280</sup>CL<sup>285</sup>GRNL<sup>290</sup>GRMEMQIMIEELSRRLPHMRLAEQ<sup>295</sup>RFDYLH  
NV<sup>300</sup>SFRAPRHLWVEWDPAQNPER<sup>305</sup>RPDI<sup>310</sup>LRLRQ<sup>315</sup>PVRIGPPRAKDVVRTMEVAAVERPSEDI  
FMN-dependent reductase  
VVLHLTRPDRRPLPRWSPGAHIDIECGEPDRS<sup>320</sup>RQ<sup>325</sup>YSLCSDPENRDAWRV<sup>330</sup>AV<sup>335</sup>Q<sup>340</sup>RD<sup>345</sup>PAS<sup>350</sup>RGG  
<sup>355</sup>SRWI<sup>360</sup>H<sup>365</sup>EEV<sup>370</sup>RP<sup>375</sup>GMLLRV<sup>380</sup>RGPRNSFRLDEHAPRYLFLAGG<sup>385</sup>IG<sup>390</sup>IT<sup>395</sup>PIMTMAARAKELGTDYEL  
HY<sup>400</sup>SV<sup>405</sup>RSRTSLIFVDEL<sup>410</sup>RQIHGDRLHVYVSEEGVRNDLAALIRRASAGTQIYAC<sup>415</sup>GP<sup>420</sup>QRMLD  
TLERLIENRPEVTLRVEH<sup>425</sup>FFGEP<sup>430</sup>SHLDPAKERPFQV<sup>435</sup>VL<sup>440</sup>RNSGLTVEVPADKTLLEVL<sup>445</sup>RAY  
Ferredoxin domain  
NIEVQSD<sup>450</sup>C<sup>455</sup>EEGL<sup>460</sup>CGT<sup>465</sup>CEVSVVEGEVDHRDSVLTRAERRENRRMM<sup>470</sup>CCCSRAKTERLVLDL<sup>779</sup>

**Red:** Heme-binding site    **Magenta:** NAD-binding site    **Blue:** FMN-binding pocket    **Orange:** [2Fe-2S]-binding site

**Figure S2.** Amino acid sequences of *T. thermophilus* CYP116B46 (NCBI: WP\_055423153).

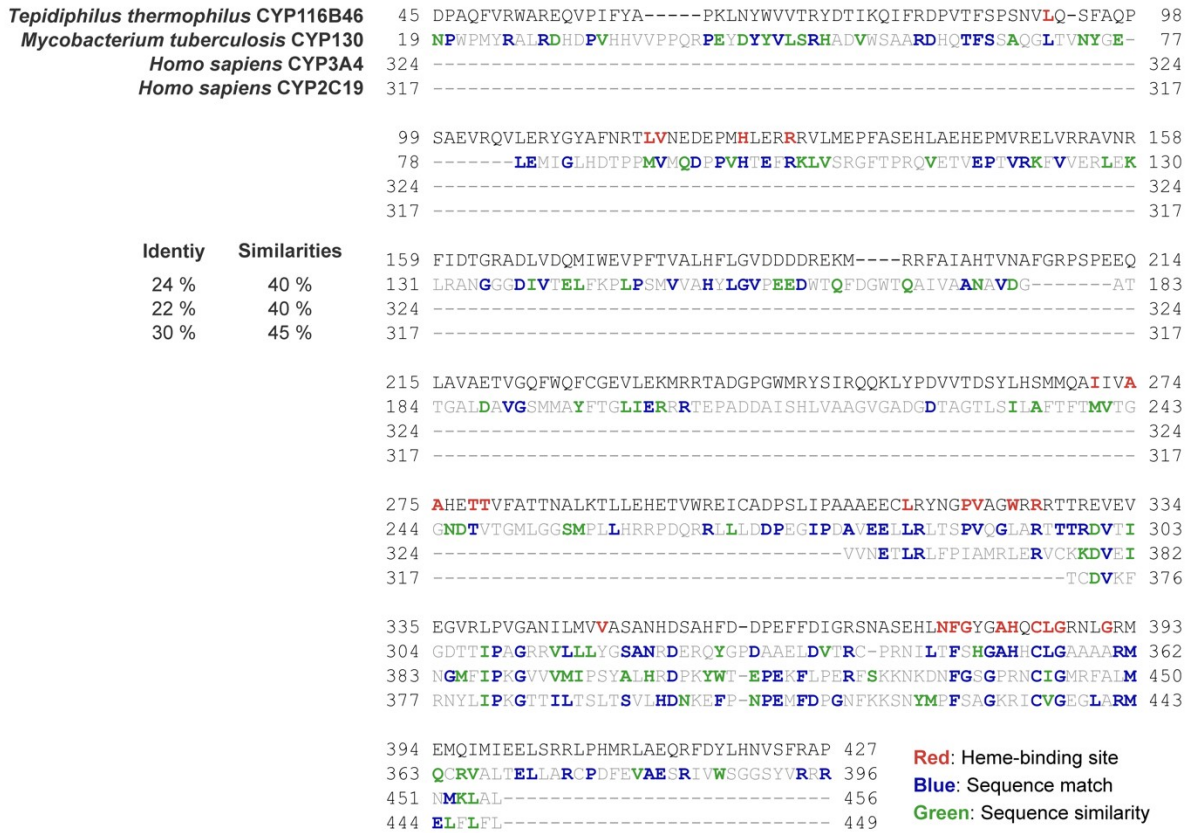


**Figure S3.** Sequence alignment of heme domain in *T. thermophilus* CYP116B46 (NCBI: WP\_055423153) with *Mycobacterium tuberculosis* CYP130 (NCBI: ALB18420.1), *Homo sapiens* CYP3A4 (NCBI: AAF13598.1), and *H. sapiens* CYP2C19 (NCBI: NP\_000760.1).



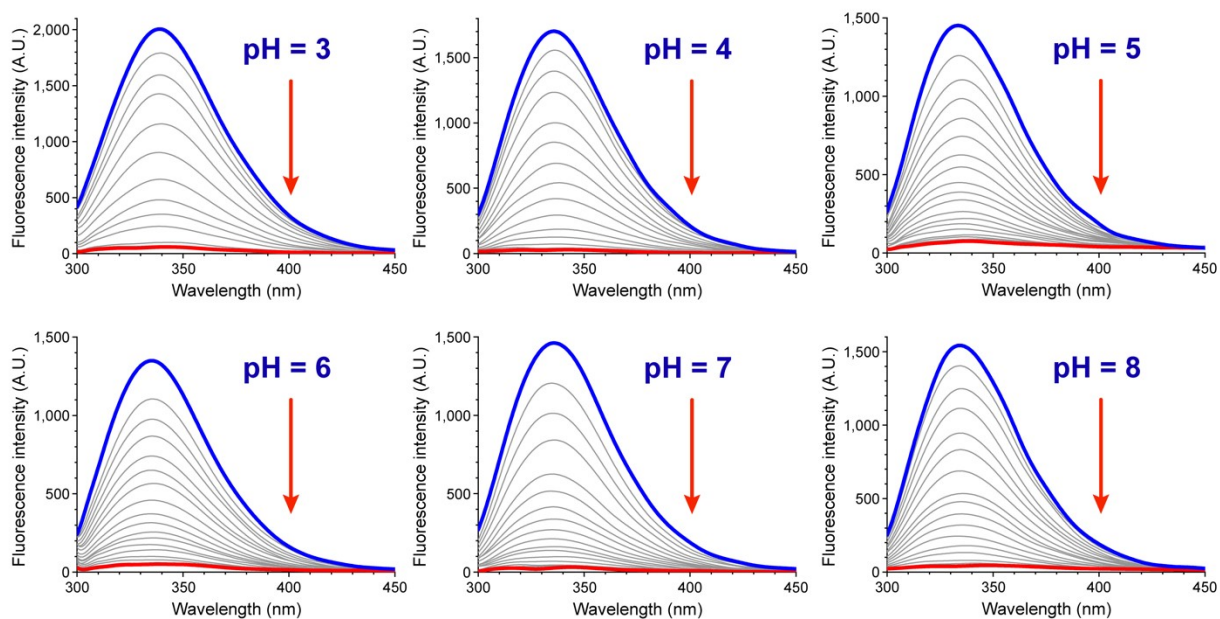


**Figure S4.** Interaction of CYP116B46 with ilaprazole based on tryptophan quenching. Conditions: [CYP116B46] = 0.32  $\mu$ M;  $\lambda_{\text{ex}}$  = 282 nm;  $\lambda_{\text{em}}$  = 332 nm; 25 mM buffer (varying pH from 3 to 8), 50 mM NaCl, 1 mM DTT; 25  $^{\circ}$ C.

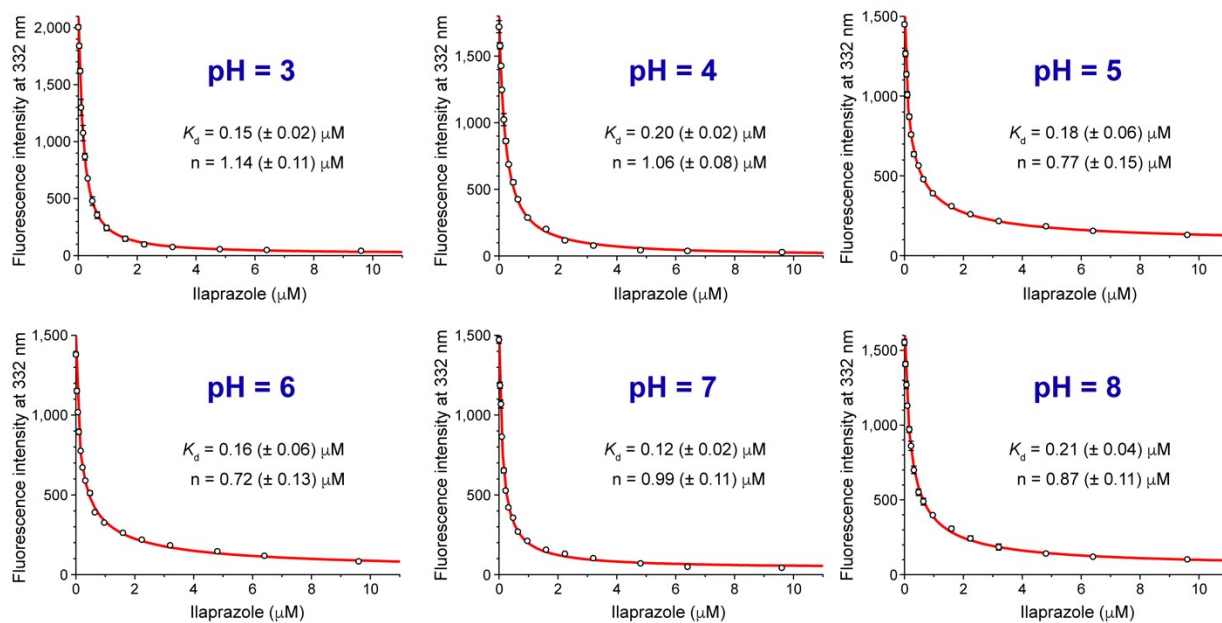


**Figure S5.** Binding affinities between CYP116B46 and ilaprazole. Dissociation constants ( $K_d$ s) were analyzed through tryptophan quenching under varying pH conditions and determined by curve fitting using the 1:n binding (Hill) equation based on fluorescence intensities at 332 nm.

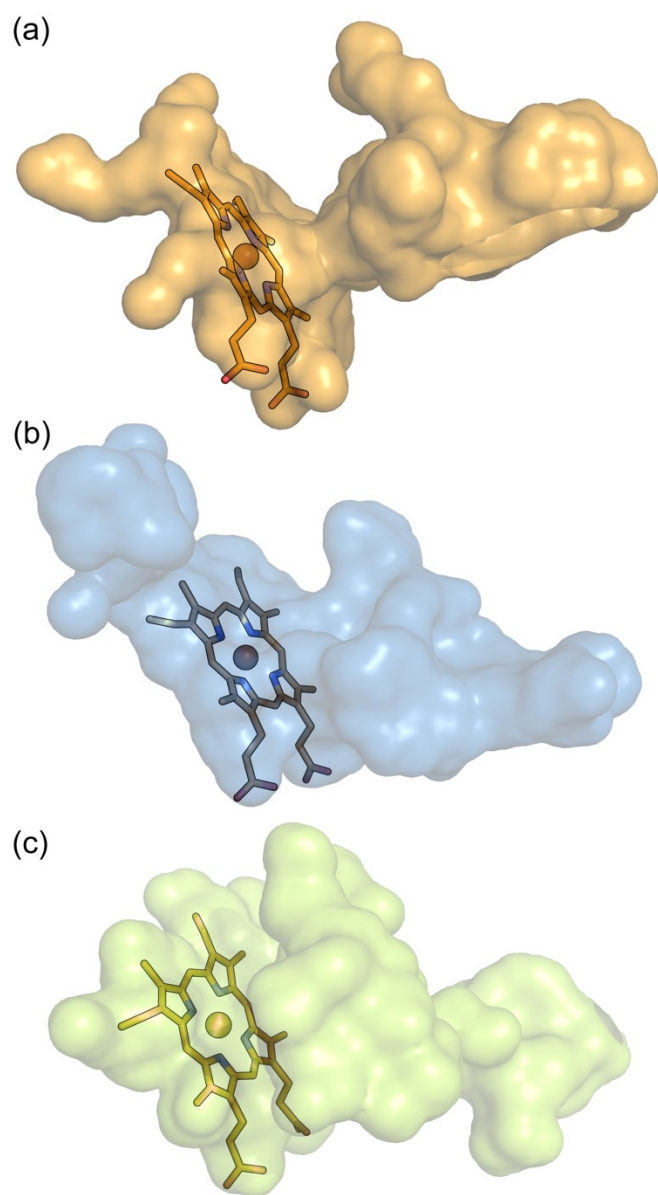


**Figure S6.** Analysis of cavities in CYP450s. The cavities were visualized using PyMOL 2.5.2 as van der Waals surfaces in the interior of (a) CYP116B46 (PDB: 6GII, orange), (b) CYP3A4 (PDB: 1TQN, skyblue), and (c) CYP2C19 (PDB: 4GQS, limon).

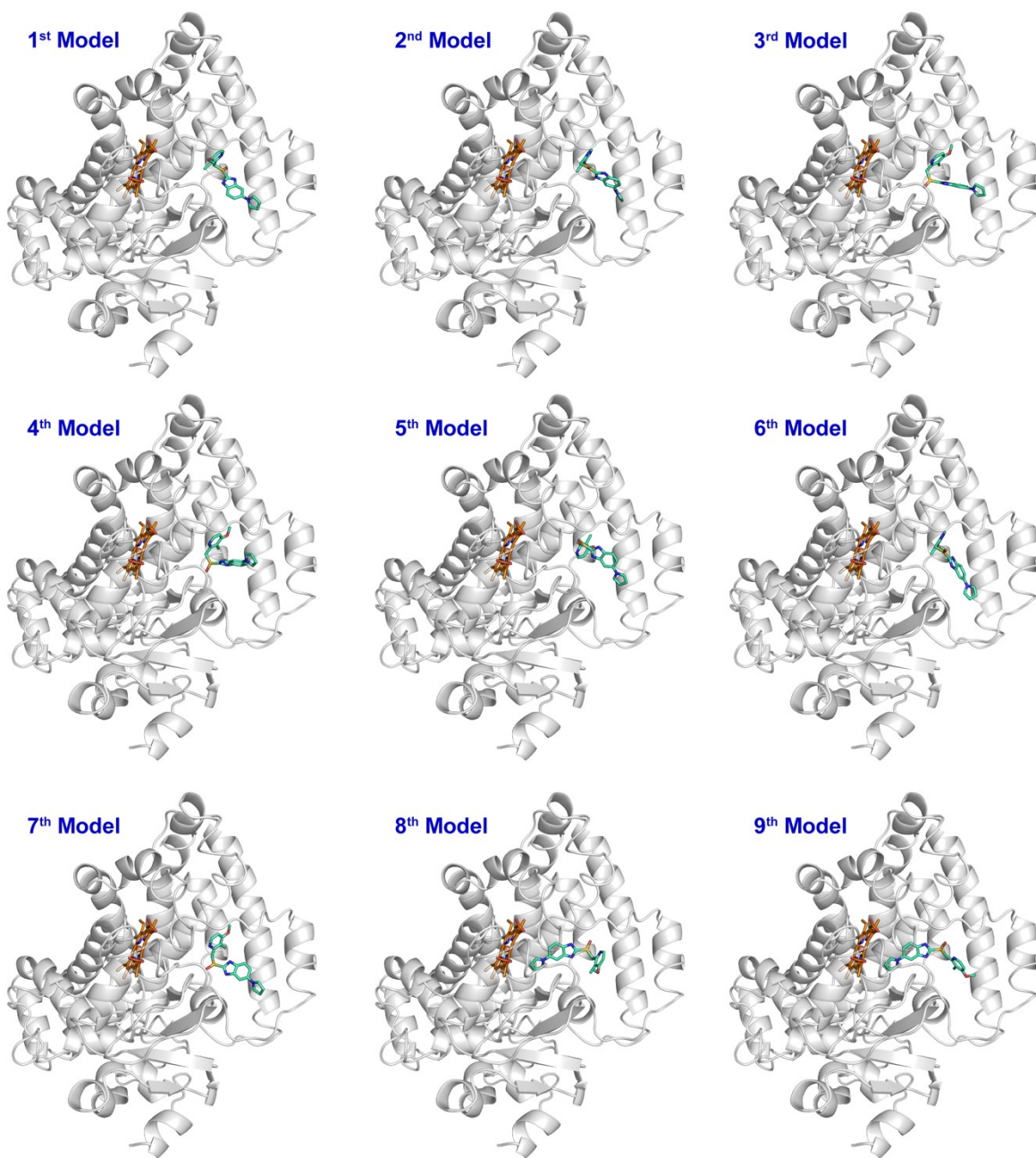


**Figure S7.** Overall docking models of CYP116B46 (PDB: 6GII) and ilaprazole.<sup>9</sup> Docking models were derived from molecular docking simulations using AutoDock Vina. The gray ribbons represent CYP116B46, orange indicates heme, and greencyan depicts ilaprazole.

**Table S1.** Binding affinities and RMSD for docking models of CYP116B46 and ilaprazole.

<b>Docking model</b>	<b>Binding energy (<math>\Delta G</math>, kcal/mol)</b>	<b>Dissociation constant (<math>K_d</math>, <math>\mu M</math>)</b>	<b>RMSD/ub</b>	<b>RMSD/lb</b>
1 <sup>st</sup> Model	-9.2	0.17	0.0	0.0
2 <sup>nd</sup> Model	-9.1	0.21	4.044	2.617
3 <sup>rd</sup> Model	-9.0	0.25	2.989	2.018
4 <sup>th</sup> Model	-9.0	0.25	4.061	3.171
5 <sup>th</sup> Model	-8.9	0.30	4.388	2.629
6 <sup>th</sup> Model	-8.8	0.35	3.604	2.258
7 <sup>th</sup> Model	-8.8	0.35	2.987	2.005
8 <sup>th</sup> Model	-8.8	0.35	8.512	4.396
9 <sup>th</sup> Model	-8.8	0.35	8.87	4.006

## References

1. N. A. Nguyen, N. T. Cao, T. H. H. Nguyen, J.-H. Ji, G. S. Cha, H.-S. Kang and C.-H. Yun, *Antioxidants*, 2021, **10**, 1327.
2. T. Omura and R. Sato, *J. Biol. Chem.*, 1964, **239**, 2379-2385.
3. A. J. Warman, J. W. Robinson, D. Luciaková, A. D. Lawrence, K. R. Marshall, M. J. Warren, M. R. Cheesman, S. E. Rigby, A. W. Munro and K. J. McLean, *FEBS J.*, 2012, **279**, 1675-1693.
4. C. Lee, S. C. Ha, Z. Rao, Y. Hwang, D. S. Kim, S. Y. Kim, H. Yoo, C. Yoon, J.-G. Na, J. H. Park and S. J. Lee, *Dalton Trans.*, 2021, **50**, 16493-16498.
5. Y. Hwang, J.-G. Na and S. J. Lee, *Appl. Environ. Microbiol.*, 2023, **89**, e02104-02122.
6. O. Trott and A. J. Olson, *J. Comput. Chem.*, 2010, **31**, 455-461.
7. I. McGonigle and S. C. Lummis, *Biochemistry*, 2010, **49**, 2897-2902.
8. J. Y. Chung, S. J. Lee, H. J. Lee, J. B. Bong, C.-H. Lee, B.-S. Shin and H. G. Kang, *J. Clin. Med.*, 2021, **10**, 2149.
9. M. Tavanti, J. L. Porter, C. W. Levy, J. R. G. Castellanos, S. L. Flitsch and N. J. Turner, *Biochem. Biophys. Res. Commun.*, 2018, **501**, 846-850.
10. W. L. DeLano, *CCP4 Newsl. Protein Crystallogr.*, 2002, **40**, 82-92.
11. J. Li, S. Dong, S. Quan, S. Ding, X. Zhou, Y. Yu, Y. Wu, W. Huang, Q. Shi and Q. Li, *Phytomedicine*, 2024, **125**, 155312.
12. J. Pu, F. Wang, W. Tang and M. Zhu, *Drug Metab. Dispos.*, 2018, **46**, 1453-1461.